

# MEF2 negatively regulates learning-induced structural plasticity and memory formation

Christina J Cole<sup>1,2,7</sup>, Valentina Mercaldo<sup>1-3,7</sup>, Leonardo Restivo<sup>1-3</sup>, Adelaide P Yiu<sup>1-3</sup>, Melanie J Sekeres<sup>1,2</sup>, Jin-Hee Han<sup>1-3,6</sup>, Gisella Vetere<sup>1-4</sup>, Tetyana Pekar<sup>1</sup>, P Joel Ross<sup>1</sup>, Rachael L Neve<sup>5</sup>, Paul W Frankland<sup>1-3</sup> & Sheena A Josselyn<sup>1-3</sup>

Memory formation is thought to be mediated by dendritic-spine growth and restructuring. Myocyte enhancer factor 2 (MEF2) restricts spine growth *in vitro*, suggesting that this transcription factor negatively regulates the spine remodeling necessary for memory formation. Here we show that memory formation in adult mice was associated with changes in endogenous MEF2 levels and function. Locally and acutely increasing MEF2 function in the dentate gyrus blocked both learning-induced increases in spine density and spatial-memory formation. Increasing MEF2 function in amygdala disrupted fear-memory formation. We rescued MEF2-induced memory disruption by interfering with AMPA receptor endocytosis, suggesting that AMPA receptor trafficking is a key mechanism underlying the effects of MEF2. In contrast, decreasing MEF2 function in dentate gyrus and amygdala facilitated the formation of spatial and fear memory, respectively. These bidirectional effects indicate that MEF2 is a key regulator of plasticity and that relieving the suppressive effects of MEF2-mediated transcription permits memory formation.

Memory formation is thought to be mediated by increases in synaptic efficacy<sup>1</sup>. As more than 90% of excitatory synapses occur on dendritic spines<sup>2</sup>, the growth and restructuring of spines may serve as a physical basis for the long-term storage of information. Consistent with this, several human cognitive disorders are characterized by abnormal dendritic spine density and morphology<sup>3</sup>. Long-term memory formation also critically depends on transcription<sup>4</sup>. Disrupting the function of several transcription factors, including nuclear factor  $\kappa$ B (NF- $\kappa$ B), cAMP response element binding protein (CREB), serum response factor (SRF) and *zif* 268 impairs memory formation, in part, by interfering with the structural plasticity required for long-term memory formation<sup>4</sup>. In this way, these transcription factors support memory formation<sup>5</sup>.

In contrast, recent studies find that MEF2 restricts activity-dependent dendritic spine growth<sup>6-8</sup>, suggesting that this transcription factor may suppress memory formation. Specifically, these studies show that increasing MEF2-mediated transcription decreases the number of dendritic spines and excitatory synapses in hippocampal neurons *in vitro*<sup>6</sup> and blocks the increase in spine density normally observed after repeated cocaine administration in rat medium spiny nucleus accumbens neurons *in vivo*<sup>8</sup>. These findings suggest that MEF2-mediated transcription negatively regulates the dendritic spine growth necessary for memory formation and that relieving the inhibitory effects of MEF2-mediated transcription may facilitate memory formation.

Here we examined the role of MEF2-mediated transcription on learning-induced dendritic spine remodeling and memory formation in adult mice. Because MEF2 is critical for neuronal survival,

differentiation and development<sup>9</sup>, we used viral vectors to manipulate MEF2 function in a temporally and spatially restricted way in the adult brain. To examine memory formation, we used two behavioral tasks that produce different types of memory and rely on distinct brain regions. First, we examined whether memory formation in mice is normally associated with changes in endogenous MEF2 levels and function. We observed that memory formation was associated with key changes in endogenous MEF2 levels and function, which would decrease MEF2-mediated transcription. Second, we assessed the effects of acutely manipulating MEF2 function on learning-induced spine remodeling and memory formation. We found that overexpressing MEF2 suppressed memory formation and that genetically relieving MEF2-mediated suppression promoted memory formation. Finally, although MEF2 may regulate the transcription of many downstream genes, we identified *Arc*, as a MEF2 target gene<sup>10</sup> that is critical for the memory-impairing effects of MEF2. *Arc* protein decreases the surface expression of AMPA-type glutamate receptors (AMPA receptors) by enhancing their endocytosis<sup>11,12</sup>. We found that the MEF2-induced disruption of memory formation was rescued by acutely interfering with AMPAR endocytosis at the time of learning. Together, these findings suggest that increasing MEF2 function impairs memory formation through an *Arc*-mediated decrease in AMPAR surface expression. These results may be interesting as MEF2 itself, as well as several of its target genes, are implicated in human cognitive or psychiatric disorders, including autism spectrum disorder<sup>13</sup>, Angelman syndrome<sup>10,14</sup> and a Rett-like syndrome with mental retardation<sup>15</sup>.

<sup>1</sup>Program in Neurosciences and Mental Health, Hospital for Sick Children, Toronto, Ontario, Canada. <sup>2</sup>Department of Physiology, University of Toronto, Toronto, Ontario, Canada. <sup>3</sup>Institute of Medical Sciences (IMS), University of Toronto, Toronto, Ontario, Canada. <sup>4</sup>Cell Biology and Neurobiology Institute, National Research Council of Italy, S. Lucia Foundation, Rome, Italy. <sup>5</sup>Brain and Cognitive Sciences, Massachusetts Institute of Technology, Cambridge, Massachusetts, USA. <sup>6</sup>Present address: Department of Biological Sciences, Korea Advanced Institute of Science and Technology, Yuseong-gu, Daejeon, Korea. <sup>7</sup>These authors contributed equally to this work. Correspondence should be addressed to S.A.J. (sheena.josselyn@sickkids.ca).

Received 18 May; accepted 9 July; published online 12 August 2012; doi:10.1038/nn.3189

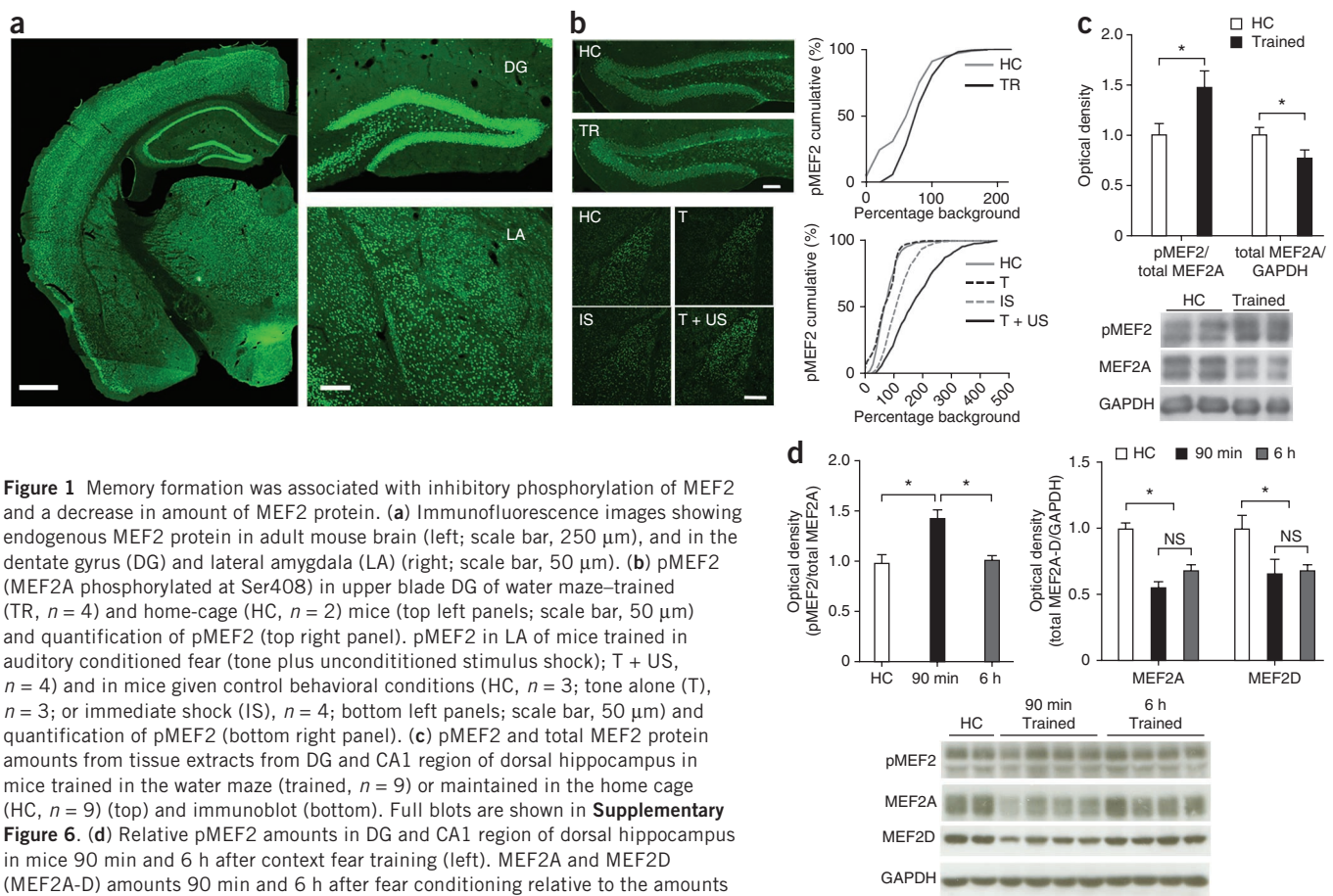


**Figure 1** Memory formation was associated with inhibitory phosphorylation of MEF2 and a decrease in amount of MEF2 protein. (a) Immunofluorescence images showing endogenous MEF2 protein in adult mouse brain (left; scale bar, 250 μm), and in the dentate gyrus (DG) and lateral amygdala (LA) (right; scale bar, 50 μm). (b) pMEF2 (MEF2A phosphorylated at Ser408) in upper blade DG of water maze-trained (TR,  $n = 4$ ) and home-cage (HC,  $n = 2$ ) mice (top left panels; scale bar, 50 μm) and quantification of pMEF2 (top right panel). pMEF2 in LA of mice trained in auditory conditioned fear (tone plus unconditioned stimulus shock; T + US,  $n = 4$ ) and in mice given control behavioral conditions (HC,  $n = 3$ ; tone alone (T),  $n = 3$ ; or immediate shock (IS),  $n = 4$ ; bottom left panels; scale bar, 50 μm) and quantification of pMEF2 (bottom right panel). (c) pMEF2 and total MEF2 protein amounts from tissue extracts from DG and CA1 region of dorsal hippocampus in mice trained in the water maze (trained,  $n = 9$ ) or maintained in the home cage (HC,  $n = 9$ ) (top) and immunoblot (bottom). Full blots are shown in **Supplementary Figure 6**. (d) Relative pMEF2 amounts in DG and CA1 region of dorsal hippocampus in mice 90 min and 6 h after context fear training (left). MEF2A and MEF2D (MEF2A-D) amounts 90 min and 6 h after fear conditioning relative to the amounts in HC mice (right). For pMEF2: HC  $n = 4$ , 90 min after fear conditioning  $n = 4$ , 6 h after fear conditioning  $n = 4$ ; for MEF2A: HC  $n = 12$ , 90 min  $n = 9$ , 6 h  $n = 9$ ; MEF2D: HC  $n = 8$ , 90 min  $n = 7$ , 6 h  $n = 7$ . Immunoblots are shown on the bottom. Full immunoblot is shown in **Supplementary Figure 6**. \* $P < 0.05$ ; NS, not significantly different. All error bars indicate s.e.m.

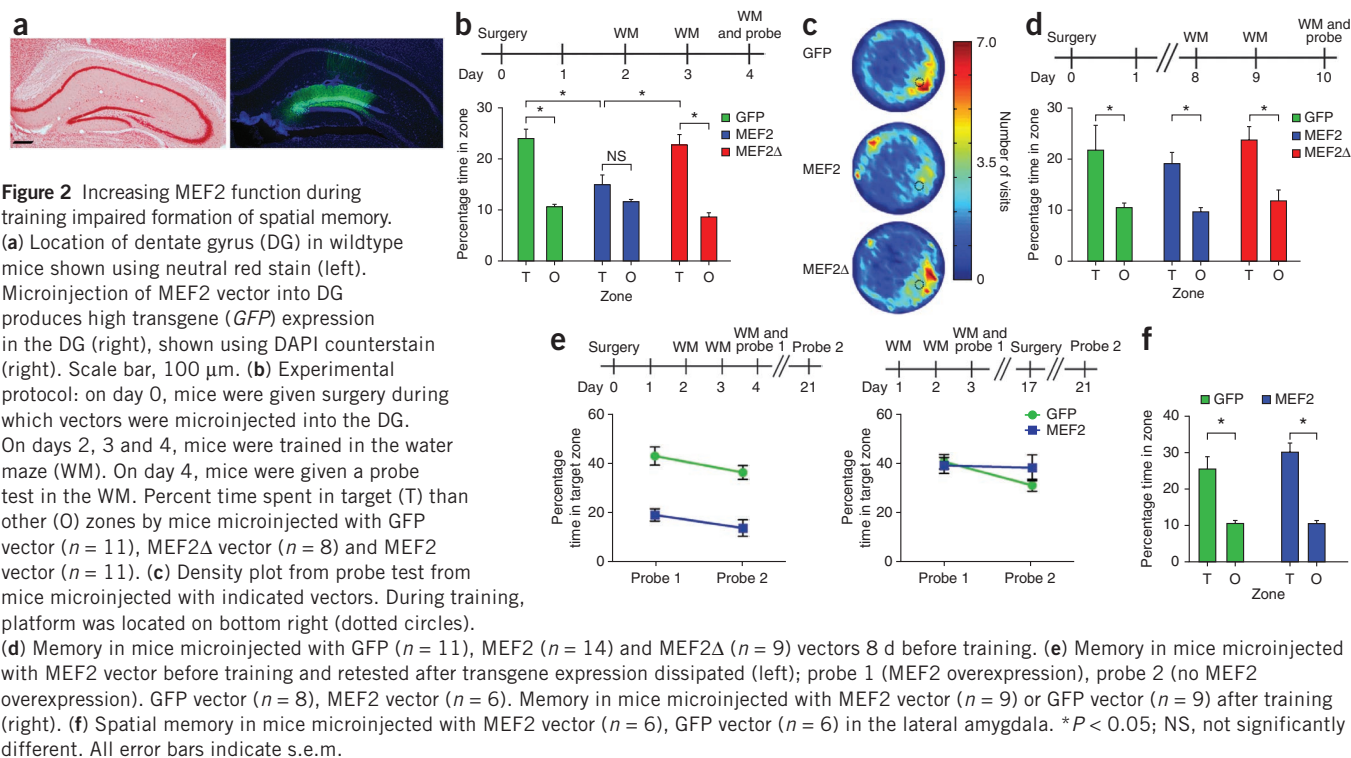
## RESULTS

### Memory formation associated with decreased MEF2 function

MEF2 proteins are endogenously expressed throughout the adult brain, including the dentate gyrus, a brain region critical for spatial memory<sup>16</sup>, and the lateral amygdala, a region critical for the acquisition of conditioned fear memory<sup>17–19</sup> (**Fig. 1a**). Whereas invertebrates have a single *mef2* gene, vertebrates, including mice and humans, have four such genes (*Mef2a–d* and *MEF2A–D*, respectively)<sup>20</sup>. The four MEF2 proteins have in common a conserved N terminus (which mediates dimerization, DNA binding and co-factor interaction) but have different C termini (which contain the transcriptional activation domain)<sup>20</sup>. MEF2A and MEF2D are the isoforms most highly expressed in forebrain regions, including the hippocampus<sup>21</sup>.

As previous results show that MEF2-mediated transcription negatively regulates spine growth, we hypothesized that memories are formed when endogenous MEF2-mediated transcription is decreased. Phosphorylation of MEF2 at a critical serine residue (Ser408 on MEF2A, which corresponds to Ser444 on MEF2D) inhibits MEF2-mediated transcription<sup>6</sup>. Accordingly, we examined whether strong behavioral training that normally produces robust memory in adult wild-type mice is correlated with phosphorylation of endogenous MEF2 at this key inhibitory site (here referred to as pMEF2). Mice trained in the water maze (using a protocol that induces robust spatial memory) exhibited significantly higher pMEF2 staining<sup>6</sup> in the dentate gyrus, particularly the upper blade of the dentate gyrus, compared to untrained mice maintained in the home cage (here referred to as

'home-cage mice') ( $P < 0.0001$ , Kolmogorov-Smirnov test; **Fig. 1b**). This finding is consistent with previous results showing that the upper blade of the dentate gyrus is particularly important in spatial memory<sup>22</sup>. Similarly, auditory fear-conditioned mice (trained with tone plus shock pairing) had significantly higher pMEF2 levels in the lateral amygdala than mice taken directly from the home cage ( $P < 0.0001$ ) or trained with either tone alone ( $P < 0.0001$ ) or an immediate shock ( $P < 0.0001$ ) (both of these control behavior procedures do not produce auditory fear memory<sup>23,24</sup>) (**Fig. 1b**). Using western blots to quantify relative pMEF2 levels (pMEF2/total MEF2), we observed similar results. Water maze-trained mice had significantly higher relative pMEF2 levels in the dentate gyrus and CA1 region of the dorsal hippocampus compared to home-cage control mice ( $F_{1,16} = 5.63$ ,  $P < 0.05$ , by one-way ANOVA; **Fig. 1c**). Water-maze training was also associated with a robust decrease in the levels of endogenous MEF2 protein ( $F_{1,16} = 5.29$ ,  $P < 0.05$ , by one-way ANOVA; **Fig. 1c**). Similarly, context fear conditioning was also associated with an increase in relative pMEF2 levels (90 min, but not 6 h, after training) and a decrease in endogenous MEF2A and MEF2D protein (90 min and 6 h after training) compared to the case in home-cage mice (MEF2A,  $F_{2,27} = 29.88$ ,  $P < 0.001$ ; MEF2D,  $F_{2,19} = 4.74$ ,  $P < 0.05$ ; **Fig. 1d**). Together, these data suggest that training which normally induces robust memory formation decreased MEF2-mediated transcription through multiple mechanisms (including a relatively short-lasting inhibitory phosphorylation of MEF2 and a longer-lasting decrease in the amount of endogenous MEF2 protein).



These findings are consistent with the interpretation that degrading endogenous MEF2 protein enables memory formation.

### Regionally and temporally specific manipulation of MEF2

We found that memory formation was associated with a decrease in MEF2-mediated transcription, leading us to predict that acutely increasing MEF2-mediated transcription at the time of training would disrupt memory formation. To test this, we locally and acutely increased MEF2 function in adult mice using replication-defective viral vectors. In the brain, endogenous MEF2 expression is limited to neurons<sup>25</sup>. Therefore, we used herpes simplex viral (HSV) vectors because HSV is neurotropic (Supplementary Fig. 1). To increase MEF2-mediated transcription, we used HSV encoding MEF2-VP16, a version of MEF2 in which the DNA-binding domain (DBD) and dimerization domain of MEF2 are fused to the transcriptional activation domain of virion protein 16 (VP16) (Supplementary Fig. 2a). MEF2-VP16 binds MEF2 sites in the promoter region of MEF2 target genes, leading to their constitutive transcription<sup>6</sup>. As a control, we used HSV encoding MEF2 $\Delta$ DBD-VP16 (MEF2 $\Delta$ ), a mutant version of MEF2-VP16 that lacks the DBD<sup>6,8</sup>. Both MEF2 and MEF2 $\Delta$  viral vectors also expressed GFP, allowing visualization of infected neurons. As an additional control, we used a vector expressing GFP alone (GFP vector). We observed no evidence of toxicity associated with these vectors (Supplementary Fig. 2b,c).

To confirm that MEF2, but not MEF2 $\Delta$ , increased MEF2-dependent transcription, we used luciferase reporter assays. Cultured cells transfected with MEF2 plasmid exhibited higher MEF2 recognition element (MRE)-dependent transcription than cells transfected with MEF2 $\Delta$  or GFP plasmid (Supplementary Fig. 2d). To examine the specificity of this increase, we infected cultured hippocampal neurons with HSV-MEF2 or control HSV-GFP and assessed both MRE- and cAMP response element (CRE)-dependent transcription under unstimulated or stimulated (4 h, 170 mM KCl) conditions. MEF2 vector increased MRE-dependent but not CRE-dependent

transcription (Supplementary Fig. 2e). Therefore, consistent with previous reports<sup>6,8</sup>, our MEF2 vector specifically increased MEF2-mediated transcription.

### MEF2 overexpression blocked formation of spatial memory

To examine the effects of acutely increasing MEF2 function on formation of spatial memory, we microinjected MEF2, MEF2 $\Delta$  or GFP vectors into the upper blade of the dentate gyrus of mice before giving them strong (six trials a day for 3 d) water-maze training<sup>26</sup>. Vector microinjection typically induced robust bilateral transgene expression specifically in the upper blade of the dentate gyrus, and we observed no differences in the extent of transgene expression in mice microinjected with different vectors (Fig. 2a). After the completion of training, we assessed spatial memory in a probe test (in which we removed the platform from the pool). Increasing MEF2 expression during training blocked the formation of spatial memory; mice microinjected with control vectors (GFP and MEF2 $\Delta$  vectors) spent more time in the area of the pool where the platform was located during training (target zone) than in other areas of the pool (other zones), whereas mice microinjected with the MEF2 vector did not show a preference for the target zone (vector  $\times$  zone  $F_{2,27} = 8.32$ ,  $P < 0.001$ , by two-way ANOVA; mice microinjected with GFP, MEF2 $\Delta$  (not MEF2) vectors searched selectively in the target zone, by *post hoc* test; confirmed by one-way ANOVA comparing target zone,  $F_{2,27} = 6.64$ ,  $P < 0.05$ ; Fig. 2b,c). Mice microinjected with MEF2 $\Delta$  vector exhibited strong spatial memory (not different from mice microinjected with GFP vector), indicating that the memory-disrupting effects resulting from microinjection of the MEF2 vector depended on the ability of MEF2 to bind DNA and activate transcription. Mice microinjected with the MEF2 vector exhibited normal latency in finding the platform during training, swim speed and thigmotaxis (tendency to swim in pool perimeter) (Supplementary Fig. 3a), indicating that increasing the amount of MEF2 did not impair motor function or swimming ability, or increase anxiety.

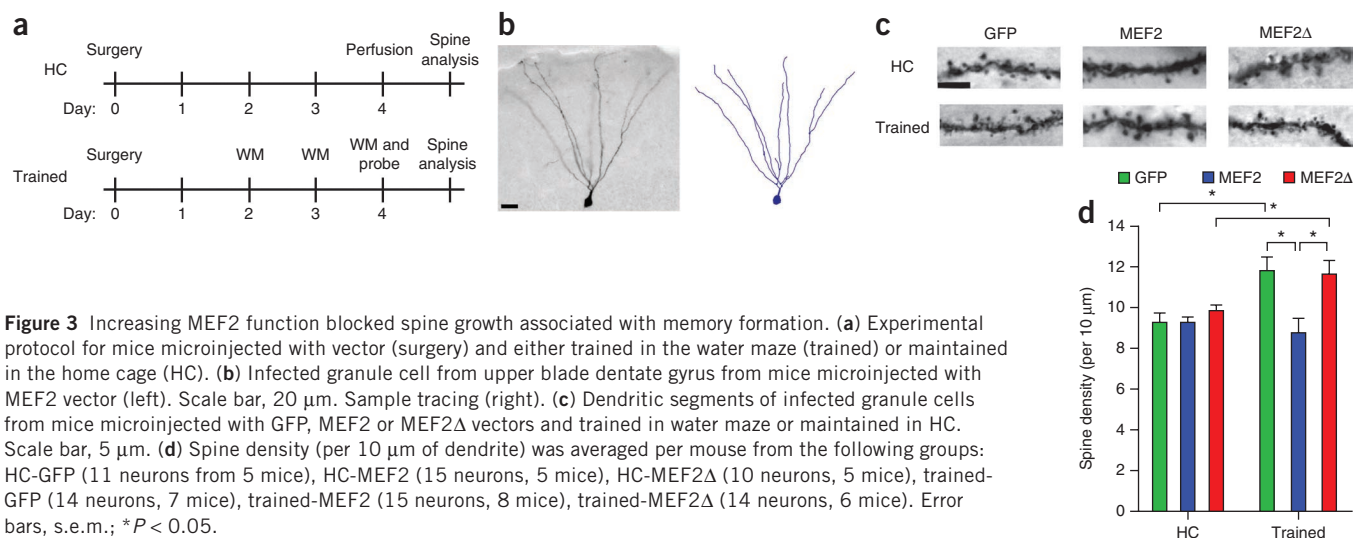


**Figure 3** Increasing MEF2 function blocked spine growth associated with memory formation. **(a)** Experimental protocol for mice microinjected with vector (surgery) and either trained in the water maze (trained) or maintained in the home cage (HC). **(b)** Infected granule cell from upper blade dentate gyrus from mice microinjected with MEF2 vector (left). Scale bar, 20  $\mu\text{m}$ . Sample tracing (right). **(c)** Dendritic segments of infected granule cells from mice microinjected with GFP, MEF2 or MEF2 $\Delta$  vectors and trained in water maze or maintained in HC. Scale bar, 5  $\mu\text{m}$ . **(d)** Spine density (per 10  $\mu\text{m}$  of dendrite) was averaged per mouse from the following groups: HC-GFP (11 neurons from 5 mice), HC-MEF2 (15 neurons, 5 mice), HC-MEF2 $\Delta$  (10 neurons, 5 mice), trained-GFP (14 neurons, 7 mice), trained-MEF2 (15 neurons, 8 mice), trained-MEF2 $\Delta$  (14 neurons, 6 mice). Error bars, s.e.m.; \* $P < 0.05$ .

It is possible that the memory impairment resulting from microinjection of the MEF2 vector was not due to an acute increase in MEF2 function during training but to a permanent disruption of hippocampal circuits. To examine this possibility, we took advantage of the relatively brief duration of transgene expression using these HSV vectors (transgene expression typically peaks roughly 2–4 d after microinjection and dissipates 8–12 d after microinjection<sup>27</sup>; **Supplementary Fig. 3b**). Therefore, we microinjected vectors into the upper blade of the dentate gyrus of mice 8 d (rather than 2 d) before training them in the water maze (**Fig. 2d**). In this experiment, we trained mice (that previously overexpressed MEF2) at a time when they were no longer overexpressing MEF2. Mice microinjected with the MEF2 vector 8 d before training subsequently exhibited strong spatial memory, which did not differ from that in mice microinjected with control vectors (MEF2 $\Delta$  and GFP vectors) (significant effect of zone only  $F_{1,31} = 23.89$ ,  $P < 0.001$ , target zone times not different between groups  $F_{2,31} = 0.47$ ,  $P > 0.05$ , by two-way ANOVA). Therefore, increasing MEF2 function during (but not over a week before) water-maze training disrupted formation of spatial memory. This finding indicates that the effects of MEF2 overexpression on memory formation were transient and not due to permanent disruption or lesion of hippocampal memory circuits.

In the experiment shown in **Figure 1b**, we microinjected the MEF2 vector 2 d before training and tested spatial memory 4 d later, at a time of MEF2 overexpression. To assess whether the poor performance on the probe trial observed in that experiment was due to increased levels of MEF2 interfering with expression (rather than formation) of spatial memory, we conducted two parallel experiments in which we disambiguated MEF2 overexpression from memory testing. First, we trained and tested mice at a time of high MEF2 expression (as in **Fig. 1b**) but retested these mice 17 d later, when viral expression of MEF2 had dissipated (**Fig. 2e**). Mice microinjected with MEF2 vector before training exhibited poor spatial memory on both the first (conducted 4 d after microinjection; MEF2 overexpression) and second (conducted 21 d after microinjection, no MEF2 overexpression) probe test compared to mice microinjected with the GFP vector (significant effect of vector  $F_{1,12} = 39.09$ ,  $P < 0.001$ , test  $F_{1,12} = 4.95$ ,  $P < 0.05$  only, by two-way ANOVA). Second, we trained and tested naive mice, and 14 d later microinjected these mice with MEF2 or GFP vector, 4 d before a probe test (**Fig. 2e**). These mice, trained when they had normal MEF2 levels, but tested

during MEF2 overexpression, exhibited normal expression of spatial memory (vector  $\times$  test  $F_{1,16} = 2.86$ , vector  $F_{1,16} = 0.02$ , test  $F_{1,16} = 4.22$ , all  $P > 0.05$ , by two-way ANOVA). Therefore, MEF2 overexpression specifically disrupted formation of spatial memory rather than expression of spatial memory.

Finally, we examined whether the disruption of the formation of spatial memory resulting from microinjection with the MEF2 vector was anatomically specific. We microinjected the MEF2 vector into the lateral amygdala, a brain region not directly implicated in the formation of spatial memory<sup>28</sup>, and observed normal formation of spatial memory (significant effect of zone  $F_{1,21} = 47.99$ ,  $P < 0.001$  only, target zone time not different between vectors  $F_{1,21} = 0.007$ ,  $P > 0.05$ ; **Fig. 2f**). Similarly, microinjection of MEF2 vector (i) outside of the upper blade of the dentate gyrus (bilateral miss) or (ii) unilaterally (rather than bilaterally) into the upper blade of the dentate gyrus (unilateral hits) (**Supplementary Fig. 3c**), also did not impair formation of spatial memory. Together, these results indicate that the memory-disrupting effects of increasing MEF2 function are both anatomically and temporally specific.

### MEF2 overexpression blocked increases in spine density

Previous studies show that increasing MEF2 function negatively regulates activity-dependent spine growth<sup>6–8</sup>. Because spine growth and remodeling may underlie memory formation, we asked whether increasing MEF2 function in the upper blade of the dentate gyrus disrupted learning-induced increases in spine density. We compared the spine density of neurons infected with MEF2 vector or GFP vector in mice trained in the water maze (from **Fig. 2b**) or maintained in the home cage (**Fig. 3a**). To visualize dendritic spines, we used a diaminobenzidine (DAB)-coupled antibody to GFP to detect the GFP expressed from each vector. This allowed us to assess the spine density across the entire neuron (rather than just dendritic segments) using bright-field conditions. GFP expression from MEF2, MEF2 $\Delta$  or GFP vectors did not differ (**Supplementary Fig. 2f,g**), all infected cells exhibited dentate gyrus granule cell morphology (**Fig. 3b**), and the overall neuronal structure or dendritic arborization did not differ between groups (**Supplementary Fig. 4a**).

Consistent with previous reports<sup>29,30</sup>, we observed that training which induces spatial memory also increased spine density in neurons infected with the control GFP vector; infected dentate gyrus granule cells from mice microinjected with GFP vector and trained

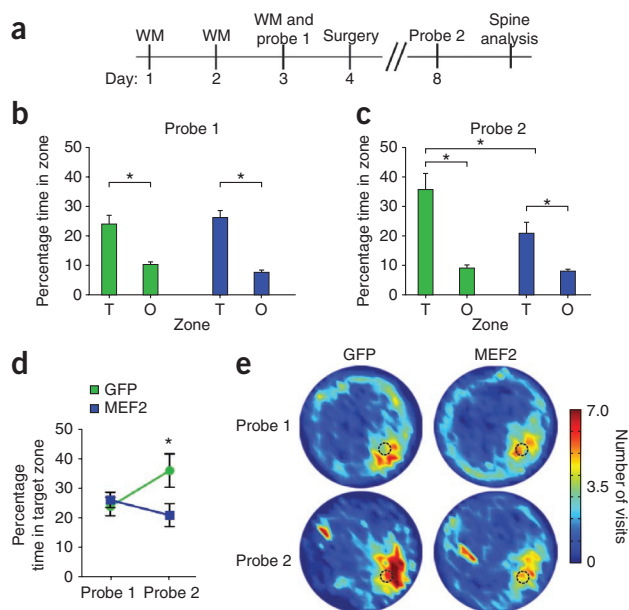


**Figure 4** Increasing MEF2 function after training impaired memory incubation. **(a)** Outline of experiment: naive mice were trained and tested in the water maze (WM and probe 1), and 24 h later, microinjected with GFP ( $n = 7$ ) or MEF2 ( $n = 9$ ) vector into upper blade of the dentate gyrus. Mice remained in home cage (without additional training) for 4 d and then tested in probe 2. After this, spine density of infected granule cells was analyzed. **(b–d)** Spatial memory was analyzed by determining percent time mice spent in target (T) zone versus other (O) zones during probe tests. Incubation is shown by mice spending more time in T zone during probe 2 than probe 1. Error bars, s.e.m.; \* $P < 0.05$ . **(e)** Density plots depicting where mice spent time during probes 1 and 2.

acquired memory<sup>31,32</sup>. Although ‘activity replay’ has been most thoroughly studied in CA1 and CA3 regions of the hippocampus, similar post-training reverberation processes may also occur in the dentate gyrus<sup>33</sup>. In the above experiments, we found that increasing dentate gyrus MEF2 function during training blocked the formation of spatial memory, perhaps by preventing spine growth. We next examined the effects of similarly enhancing MEF2 function shortly after water-maze training on post-training memory processing and related spine remodeling.

We trained naive mice in the water maze and microinjected MEF2 or GFP vector into the upper blade of the dentate gyrus 24 h after an initial probe test (Fig. 4a). As expected, all mice had intact spatial memory according to this initial probe test (probe 1; Fig. 4b). Then we microinjected these mice with MEF2 or GFP vectors and returned them to their home cage for 4 d, without additional training (probe 2). In the second probe test, mice with GFP vector exhibited enhanced spatial memory (spending more time in the target zone during probe 2 than probe 1), similar to the case in memory incubation<sup>34</sup>. In contrast, mice with MEF2 vector did not exhibit enhanced spatial memory in the second probe test (vector  $\times$  test interaction  $F_{1,14} = 13.39$ ,  $P < 0.05$ , two-way ANOVA; mice microinjected with GFP vector spent significantly more time in target zone rather than other zone during probe 2 than probe 1,  $P < 0.05$ , whereas mice with MEF2 vector did not show this increase during probe 2,  $P > 0.05$ , *post hoc* test; (Fig. 4b–e). This suggests that overexpressing MEF2 prevented this incubation-like memory enhancement. We examined the spine density of infected dentate granule cells in these mice (after probe 2). Consistent with the absence of memory enhancement, mice with MEF2 vector had lower spine density than mice with GFP vector (spine density (mean spine number per 10  $\mu\text{m}$  dendrite length  $\pm$  s.e.m.) for GFP vector,  $12.76 \pm 0.16$ ; MEF2 vector,  $10.77 \pm 0.25$ ;  $F_{1,10} = 48.45$ ,  $P < 0.001$ , one-way ANOVA). Together, these results suggest that increasing MEF2 function interfered with a post-training process that resembles memory incubation and requires spine growth.

### MEF2 overexpression in amygdala blocked fear memory

Increasing MEF2 function in the upper blade of the dentate gyrus during water-maze training impaired formation of spatial memory. To assess whether the role of MEF2 was conserved across brain region and type of memory, we similarly microinjected vectors into the lateral amygdala before strong conditioned fear training (one tone plus shock pairing with 0.5-mA shock) and examined contextual and discrete tone fear memory 24 h and 48 h later, respectively (Fig. 5a,b). Overexpressing MEF2 in the lateral amygdala during training blocked the formation of long-term fear memory for context fear ( $F_{2,19} = 6.37$ ,  $P < 0.05$ ; Fig. 5c) and tone fear ( $F_{2,19} = 4.50$ ,  $P < 0.05$ ; Fig. 5d). Mice with MEF2 vector froze less than mice with MEF2 $\Delta$  or GFP vector in both fear memory tests. Consistent with the role of the dentate gyrus in context fear memory but not

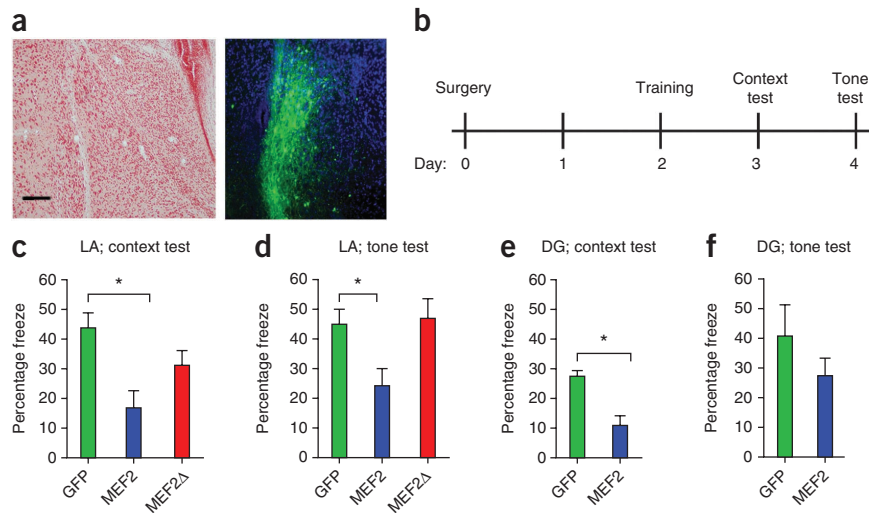
in the water maze (GFP-trained mice) exhibited greater spine density than infected dentate gyrus granule cells from mice microinjected with GFP vector and maintained in the home cage (GFP-home cage mice) (Fig. 3c,d). This training-induced increase in spine density was blocked by overexpressing MEF2 (spine density of infected neurons from MEF2-trained mice did not differ from infected neurons from GFP-home-cage mice and was lower than infected neurons from GFP-trained mice). MEF2 vector had no effect on spine density in home-cage mice, consistent with reports that MEF2 specifically inhibits activity-dependent spine growth<sup>6,8</sup>. Finally, spine density in neurons with MEF2 $\Delta$  vector did not differ from that in neurons with GFP vector, in either trained or home-cage mice. This interpretation was supported by the results of a two-way ANOVA, which showed a significant vector  $\times$  condition interaction  $F_{2,30} = 3.61$ ,  $P < 0.05$ , and main effects of vector  $F_{2,30} = 4.99$ ,  $P < 0.05$  and condition  $F_{1,30} = 6.44$ ,  $P < 0.05$ . *Post hoc* Newman-Keuls comparisons revealed spine density in infected neurons from GFP-trained  $>$  GFP-home cage,  $P < 0.05$ , GFP-trained  $>$  MEF2-trained,  $P < 0.05$ , MEF2-trained = GFP-home cage = MEF2-home cage,  $P > 0.05$  and MEF2-home cage = GFP-home cage,  $P > 0.05$ . Therefore, acutely increasing MEF2 function prevented the spine growth normally observed with formation of spatial memory. This repression of spine growth depended on both neural activity (lack of effect in home-cage mice) and MEF2-mediated transcription (lack of effect with MEF2 $\Delta$  vector). As memory formation is thought to require spine remodeling, this prevention of spine growth may account for the memory-disruptive effects of increasing MEF2 function. It is interesting to note that introduction of the MEF2 vector resulted in not only inhibition of spine growth in MEF2-infected dentate gyrus cells but also in neighboring non-infected dentate gyrus cells (Supplementary Fig. 4b,c), suggesting that increasing MEF2 function inhibited spine growth and memory formation in a circuit rather than in a cell-autonomous manner.

### MEF2 overexpression after training prevented memory incubation

Activation of hippocampal circuits during training is critical for the formation of spatial memory. Similarly, reactivation of hippocampal circuits after training may be important for strengthening a previously

**Figure 5** Overexpressing MEF2 in the lateral amygdala blocked long-term memory formation for contextual and cued fear conditioning.

(a) Location of lateral amygdala (left); stained with neutral red. Scale bar, 400  $\mu$ m. Transgene (*GFP*) expression (right; green) after microinjection of MEF2 vector into the lateral amygdala. Sample was counterstained with DAPI (blue). (b) Outline of experimental protocol: mice were microinjected with vector and 2 d later, trained for tone fear conditioning (one tone plus shock pairing, 0.5-mA shock). Mice were tested for context and tone-fear memory 24 h and 48 h later, respectively. (c) In the context test, mice with MEF2 vector in the lateral amygdala (LA) ( $n = 8$ ) spent less time freezing than mice with control vectors (*GFP* vector,  $n = 7$ ; MEF2 $\Delta$  vector,  $n = 7$ ), which did not differ from each other. (d) In the tone test, mice with MEF2 vector froze less than mice with either control vector. (e,f) Context and tone fear memory with microinjection of indicated vectors in the dentate gyrus (DG) before fear conditioning. Mice with MEF2 vector ( $n = 8$ ) in upper blade of the DG froze less than mice with *GFP* vector ( $n = 7$ ) in context test. Groups froze equally during tone test. All error bars indicate mean  $\pm$  s.e.m.; \* $P < 0.05$ .



tone fear memory, we also observed that mice microinjected with MEF2 vector in the upper blade of the dentate gyrus exhibited disrupted context fear memory ( $F_{1,10} = 19.31$ ,  $P < 0.05$ ; **Fig. 5e**) but intact tone fear memory ( $F_{1,10} = 0.15$ ,  $P > 0.05$ ; **Fig. 5f**). In contrast to the effects on long-term memory, microinjecting MEF2 vector in the lateral amygdala did not disrupt tone fear memory, as assessed 90 min after training (mean percentage time spent freezing  $\pm$  s.e.m. for mice with *GFP* vector,  $31.34 \pm 3.72$ ,  $n = 7$ ; and with MEF2 vector,  $28.72 \pm 4.18$ ,  $n = 7$ ;  $P > 0.05$ ). Together, these findings show that increasing MEF2 function impaired formation of a long-term but not short-term memory. Because the disruptive effects of increasing MEF2 function on memory formation were not exclusive to a particular brain region (dentate gyrus or lateral amygdala) or type of memory (spatial or fear), these results indicate that MEF2 has a conserved role in the formation of memory.

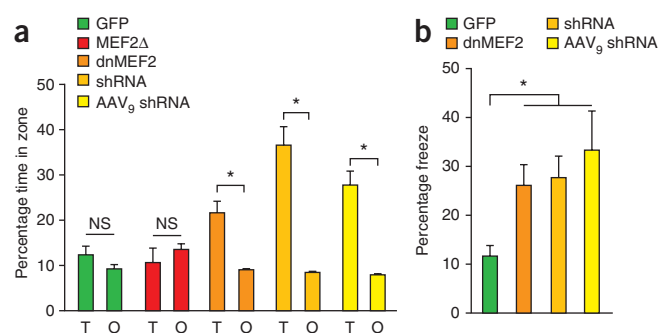
### Disrupting MEF2 function permitted formation of memory

We observed that formation of memory in normal, intact mice was associated with inhibitory phosphorylation of MEF2 and decreased amounts of MEF2A and MEF2D protein, suggesting that endogenous MEF2-mediated transcription normally constrains memory formation. Therefore, we asked whether acutely decreasing MEF2 levels during training would enhance memory formation. To disrupt MEF2-mediated

transcription, we used several complementary strategies. First, we used HSV to express either a dominant-negative form of MEF2 (dnMEF2; **Supplementary Fig. 2a**) or short-hairpin RNA (shRNA) against *Mef2a* and *Mef2d*. We verified that these shRNAs robustly decreased levels of endogenous MEF2A and MEF2D proteins (**Supplementary Fig. 5a,b**). Second, we used AAV<sub>9</sub> to express different shRNAs that had been previously used to knock down *Mef2a* and *Mef2d* *in vitro* and *in vivo*<sup>6,8,21</sup>. To examine whether disrupting MEF2 function enhanced memory, we trained mice under weak training conditions that are not normally sufficient to support robust memory formation.

First, we examined spatial memory by ‘weakly’ training mice in the water maze (three trials a day for 3 d, half the number of training trials used previously) after microinjection of vector into the upper blade of the dentate gyrus. Consistent with previous results<sup>26</sup>, this weak training was not sufficient to support formation of spatial memory in mice with control vectors (*GFP* or MEF2 $\Delta$ ) (mice searched equally in the target and other zones during the probe test). In contrast, mice with disrupted MEF2 function (HSV-dnMEF2, HSV-shRNA to *Mef2a* and *Mef2d* or AAV<sub>9</sub>-shRNA vectors) exhibited robust spatial memory, searching selectively in the target zone (significant vector  $\times$  zone interaction  $F_{4,49} = 12.08$ ,  $P < 0.001$ , *post hoc* tests confirmed that only mice with HSV-dnMEF2, HSV-shRNA or AAV<sub>9</sub>-shRNA vector searched preferentially in target zone; mice with HSV-dnMEF2,

**Figure 6** Disrupting MEF2 function permitted robust memory formation after weak training. (a) Mice were microinjected with HSV vectors expressing *GFP*, MEF2 $\Delta$ , dnMEF2 or shRNA against *Mef2a* and *Mef2d* or AAV<sub>9</sub> expressing different shRNA against *Mef2a* and *Mef2d* into upper blade of the dentate gyrus before weak water-maze training (three trials per day for 3 d). Weak training was not sufficient to support formation of spatial memory in mice with control vectors (*GFP* vector ( $n = 13$ ) or MEF2 $\Delta$  vector ( $n = 7$ )); mice spent similar time searching in target (T) and other (O) zones. Weak training was sufficient to induce robust formation of spatial memory in mice with decreased MEF2 function (HSV-dnMEF2 ( $n = 17$ ), HSV-shRNA ( $n = 7$ ) or AAV<sub>9</sub>-shRNA ( $n = 10$ ) vector). (b) Mice were microinjected with HSV vectors expressing *GFP*, dnMEF2 or shRNA against *Mef2a* and *Mef2d* or AAV<sub>9</sub> expressing shRNA against *Mef2a* and *Mef2d* into lateral amygdala before weak fear conditioning training (one tone plus shock pairing, 0.3-mA shock). Mice microinjected with dnMEF2 vector ( $n = 9$ ), HSV-shRNA ( $n = 6$ ) or AAV<sub>9</sub>-shRNA ( $n = 9$ ) froze more than mice with *GFP* vector ( $n = 14$ ) during tone fear test. All error bars indicate s.e.m. \* $P < 0.05$ ; NS, not significantly different.



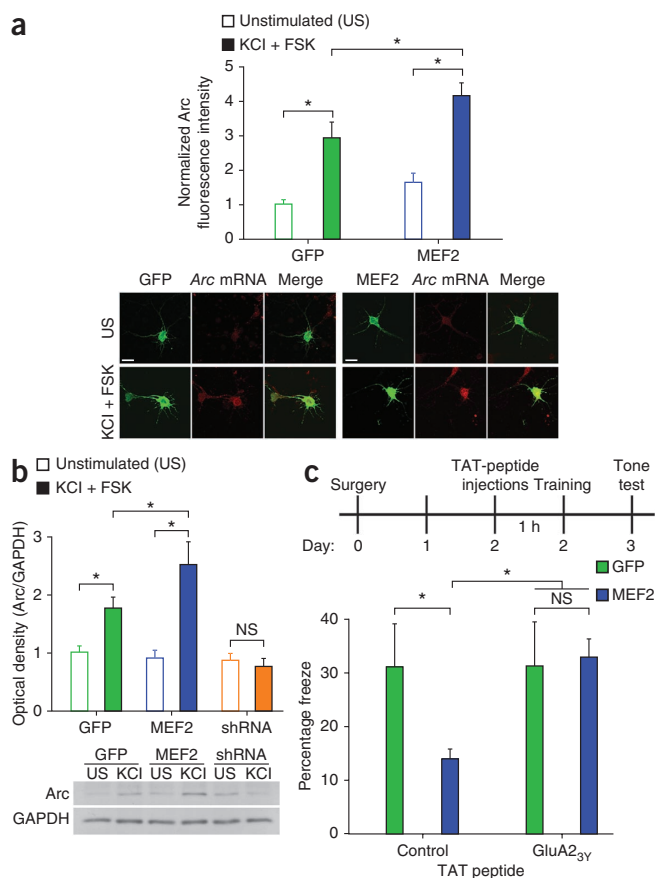


**Figure 7** Memory disruption produced by increasing MEF2 rescued by disrupting AMPAR endocytosis. **(a)** Amount of *Arc* mRNA (normalized intensity of fluorescence *in situ* hybridization signal for probe against *Arc* mRNA) in primary hippocampal neurons transfected with GFP plasmid or MEF2 plasmid, and unstimulated or stimulated with KCl + forskolin (FSK). Representative images of primary neurons expressing GFP plasmid (left) or MEF2 plasmid (right) showing staining for GFP (transfected with plasmid, GFP, green) and *Arc* mRNA (red) both in an unstimulated (US) condition and after KCl + FSK stimulation. Scale bars, 20  $\mu$ m. **(b)** Amount of Arc protein (Arc/GAPDH optical intensity) in primary hippocampal neurons infected with GFP vector or MEF2 vector, and unstimulated or stimulated with KCl + FSK. Immunoblot (bottom); full immunoblot is shown in **Supplementary Figure 6**. **(c)** Mice microinjected with MEF2 or GFP vector in lateral amygdala were administered TAT-GluA2<sub>3Y</sub> or TAT control peptide before auditory fear conditioning ( $n = 8$  for all groups). All error bars indicate s.e.m.; \* $P < 0.05$ ; NS, not significantly different.

the expression of several target genes<sup>10</sup>. We focused on the MEF2 target gene *Arc*<sup>6,10</sup> because Arc protein is implicated in synaptic function and memory<sup>35</sup>. Consistent with previous findings, we observed that our MEF2 vector robustly increased the amounts of Arc RNA ( $F_{3,129} = 14.94$ ,  $P < 0.001$ ; **Fig. 7a**) and protein (**Fig. 7b**). Previous findings indicate that neuronal activity increases Arc expression at activated dendritic regions<sup>35</sup>. We observed that viral expression of shRNA against *Mef2a* and *Mef2d* also prevented the activity-induced increase in the amount of Arc protein (significant vector  $\times$  stimulation interaction  $F_{2,46} = 7.86$ ,  $P < 0.001$ , vector  $F_{2,46} = 8.74$ ,  $P < 0.001$ , stimulation  $F_{1,46} = 20.67$ ,  $P < 0.001$ ; **Fig. 7b**).

Arc reduces the amplitude of synaptic currents mediated by AMPARs by promoting their endocytosis<sup>11,12,36</sup>. AMPARs are composed of four subunit types (GluR1–4 or GluA1–4), which combine to form tetramers<sup>37</sup>. In mature hippocampal pyramidal neurons, most AMPARs consist of GluA1–GluA2 or GluA2–GluA3 heterodimers<sup>37</sup>. Endocytosis of GluA2-containing AMPARs decreases synaptic efficacy and is critical for the expression of some forms of long-term depression (a rapid form of synaptic plasticity characterized by a decrease in synaptic strength and dendritic spine size or density)<sup>37,38</sup> and homeostatic synaptic scaling (a slower form of plasticity in which the total synaptic strength of a neuron is modified to regulate neuronal excitability)<sup>39</sup>. Arc may preferentially enhance internalization of GluA2-containing AMPARs<sup>36</sup>. Together, these findings suggest that MEF2 may disrupt memory formation by increasing Arc expression, which would decrease surface expression of GluA2-containing AMPAR. Therefore, we tested whether interfering with GluA2-containing AMPAR endocytosis during training prevented the memory deficits induced by overexpressing MEF2.

To disrupt GluA2-containing AMPAR endocytosis, we used an interference peptide (GluA2<sub>3Y</sub>) that blocks activity-dependent endocytosis of GluA2-containing AMPARs<sup>40</sup>. Fusing GluA2<sub>3Y</sub> peptide to a TAT protein transduction domain allows this peptide to enter the brain; systemic injection of TAT-GluA2<sub>3Y</sub> peptide produces robust behavioral effects in animal models of addiction<sup>40</sup>. We microinjected mice with MEF2 or GFP vectors in the lateral amygdala as above, and 60 min before auditory fear training, systemically administered TAT-GluA2<sub>3Y</sub> or a control (TAT alone) peptide. Consistent with our previous findings (**Fig. 5d**), mice with MEF2 vector (and control peptide) exhibited impaired formation of tone fear memory. However, administering TAT-GluA2<sub>3Y</sub> peptide before training was sufficient to rescue the MEF2-induced memory deficit (**Fig. 7c**). That is, mice with MEF2 vector but injected with TAT-GluA2<sub>3Y</sub> peptide froze at high levels during the tone memory test (freezing levels did not differ from control mice with GFP vector; significant vector  $\times$  TAT peptide interaction  $F_{1,28} = 4.26$ ,  $P < 0.05$ ; *post hoc* tests showed that mice with MEF2 vector plus

HSV-shRNA or AAV<sub>9</sub>-shRNA vector spent more time in target zone than mice with either GFP or MEF2 $\Delta$  vector, which did not differ from each other  $F_{4,49} = 10.24$ ,  $P < 0.001$ ; **Fig. 6a**). Thus, decreasing MEF2 function via exogenous expression of dnMEF2 or via shRNA-mediated knockdown was sufficient to produce strong spatial memory after subthreshold training.

Second, we observed that decreasing MEF2 levels in the lateral amygdala facilitated the formation of auditory fear memory. We microinjected HSV expressing GFP, dnMEF2, shRNA against *Mef2a* and *Mef2d* or AAV<sub>9</sub> expressing shRNA (as above) into the lateral amygdala before weak fear training (one tone plus shock pairing with 0.3-mA shock). As expected using these weak training conditions, mice with control vector (HSV-GFP) showed low fear memory during the tone fear test. However, mice with disrupted MEF2 function (HSV-dnMEF2, HSV-shRNA or AAV<sub>9</sub>-shRNA) froze at high levels during the tone fear test, showing robust fear memory after this weak fear training ( $F_{3,34} = 4.79$ ,  $P < 0.001$ , *post hoc* tests showed that HSV-dnMEF2, HSV-shRNA or AAV<sub>9</sub>-shRNA groups froze more than mice microinjected with GFP vector; **Fig. 6b**). Therefore, using two paradigms that produce different types of memory, we found that weak training was sufficient to induce strong memory formation if, and only if, MEF2 function was disrupted. Together, these results indicate that MEF2 acts as an endogenous molecular brake on memory formation. Relieving the MEF2-inhibitory constraint facilitated memory formation.

### Memory impairment rescued by targeting AMPAR endocytosis

Our results showed that increasing MEF2 function disrupted memory formation. We next explored a possible molecular mechanism underlying this effect. MEF2 is a transcription factor that regulates

control peptide showed lower freezing than mice with GFP vector plus control peptide, but that mice with MEF2 vector plus GluA2<sub>3Y</sub> peptide showed similar levels of freezing to mice with GFP vector plus control peptide. Injection of TAT-GluA2<sub>3Y</sub> peptide had no effect on memory formation in mice with control GFP vector, in agreement with previous reports<sup>41</sup>. These findings are consistent with the interpretation that MEF2 disrupts memory formation by increasing Arc expression, which, in turn, decreases surface expression of AMPARs.

## DISCUSSION

Based on previous findings that MEF2 negatively regulates spine growth, we hypothesized that MEF2-mediated transcription normally inhibits memory formation. We found that strong training (sufficient to induce either robust fear or formation of spatial memory) was associated with phosphorylation of endogenous MEF2 at a site that inhibits MEF2-mediated transcription as well as decreased levels of MEF2A and MEF2D protein. These observations are consistent with the notion that MEF2-mediated transcription negatively regulates memory formation. We found that overexpressing MEF2 specifically during training blocked spatial and fear memory formation, in a brain region-dependent manner. Increasing MEF2 function also prevented the increase in spine density normally associated with formation of spatial memory, suggesting that MEF2-mediated transcription constrains memory formation by interfering with the required underlying structural plasticity. In contrast, we also found that relieving the suppressive effects of MEF2-mediated transcription (expressing dnMEF2 or knocking down endogenous MEF2A and MEF2D) was sufficient to produce robust spatial or fear memory under weak training conditions that were not normally sufficient to support memory formation. Finally, we examined a potential mechanism mediating the memory deficits induced by overexpressing MEF2. Consistent with previous results, we found that increasing MEF2 amounts increased Arc expression. As Arc decreases AMPAR-mediated synaptic currents by promoting AMPAR endocytosis, we investigated whether the memory deficits induced by MEF2 could be prevented by interfering with AMPAR endocytosis at the time of training. We found that administering a peptide that disrupts AMPAR endocytosis completely restored the memory deficit induced by MEF2 overexpression. Together, our results identified *Mef2* as a memory suppressor gene that may disrupt memory formation through the synaptic protein Arc to decrease the surface expression of AMPAR.

We locally and acutely manipulated MEF2 function in the adult brain, rather than chronically throughout development because MEF2 is required for neuronal survival and differentiation<sup>9</sup>. For instance, inducible deletion of *Mef2c* at an early developmental stage (floxed *Mef2c* mice crossed with mice in which Cre recombinase is driven by the nestin promoter) produces transgenic mice with both abnormal neuronal aggregation and synaptic transmission<sup>42</sup>. Similar deletion of *Mef2c* at a later developmental stage (Cre recombinase driven by *GFAP* promoter) produces adult transgenic mice that may have developmental neurological deficits (mice have reduced body weight, impaired beam walking and an abnormal clasp reflex)<sup>7</sup>. As might be expected by decreasing MEF2 function, these transgenic mice with a deletion of *Mef2c* show increased dendritic spine density in dentate gyrus neurons. However, these mice also show disrupted context fear memory, perhaps because of developmental neurological deficits. In contrast, transgenic mice that chronically express MEF2-VP16 across many brain regions (driven by *NSE* promoter) show decreased dentate gyrus spine density but normal context-fear memory<sup>7</sup>. Although these studies clearly demonstrate the importance of MEF2 during development, they do not allow the role of MEF2

in development versus adult memory formation to be clearly distinguished. Therefore, to specifically examine the role of MEF2 in adult memory formation, we manipulated MEF2 function in a spatially and temporally restricted manner. In addition to the importance of MEF2 in development, our data show that MEF2 is also important in adult memory formation.

We found that increasing MEF2 function in the upper blade of the dentate gyrus prevented formation of spatial memory. This memory-formation impairment was specific in several ways. First, the memory disruption resulting from the introduction of our MEF2 vector depended on MEF2-mediated transcription as similar microinjection of a MEF2Δ vector (encoding MEF2 lacking a DBD, which cannot activate transcription) did not impair memory formation. Second, formation of spatial memory was impaired only when MEF2 function was increased during water-maze training and not 1 week before or over 2 weeks after training. These findings indicate that the effects of increasing MEF2 function are reversible and that increasing MEF2 function did not impair expression of a previously acquired memory. Third, the effects of MEF2 on formation of spatial memory were anatomically specific. In fact, we observed a double dissociation between the effects of increasing MEF2 function in the dentate gyrus versus lateral amygdala on the formation of different types of memory. Microinjecting MEF2 vector in the upper blade of the dentate gyrus impaired spatial memory while leaving tone-fear memory intact, whereas microinjecting MEF2 vector into lateral amygdala disrupted the formation of fear memory but not of spatial memory. Tests of spatial and fear memories differ along several dimensions (including performance demands, sensory features, content of learning, amount of training required for memory formation, brain regions critically involved and other factors). The finding that overexpressing MEF2 disrupted the formation of both types of memory suggests that it is unlikely that MEF2 vector impaired general behavioral performance. Rather, these data indicate that MEF2 has a general role in regulating memory formation that is conserved across brain region and type of memory.

We observed that memory formation was accompanied by an increase in dendritic spine density in hippocampal granule cells, consistent with previous data<sup>29,30</sup>. Spines, first described over 100 years ago<sup>43</sup>, are hypothesized to serve as a physical substrate of long-term memory<sup>1,3,43</sup>. MEF2 restricts the number of excitatory synapses and spine growth across several preparations and species (including *Caenorhabditis elegans* excitatory neuromuscular junction synapses<sup>44</sup>, rat hippocampus neurons *in vitro*<sup>6</sup>, mouse hippocampus neurons *in vivo*<sup>7</sup> and rat nucleus accumbens neurons *in vivo*<sup>8</sup>). Here we found that acutely overexpressing MEF2 prevented the increase in spine density that normally accompanies formation of spatial memory. Consistent with the activity-dependent mechanism previously described in other systems, increasing MEF2 did not decrease spine density in home cage control mice. Therefore, MEF2 has a conserved role in structural plasticity in response to diverse neuronal activity.

Memory incubation, the enhancement of memory over time in the absence of additional training, is observed across several behavioral paradigms<sup>23,45</sup>. However, little is known about the mechanisms underlying incubation. One possibility is that post-training reactivation of activity patterns that occurred during training<sup>31,32</sup> contributes to incubation by promoting spine growth and strengthening neural circuits. We examined this possibility by overexpressing MEF2 in the upper blade of the dentate gyrus 1 d after water-maze training. Mice microinjected with control GFP vector exhibited an incubation-like effect (enhanced spatial memory on a second probe test, conducted without additional training). In contrast, mice microinjected with

MEF2 vector after training did not exhibit enhanced memory on the subsequent memory test, suggesting that increasing MEF2 function prevented memory incubation. Moreover, the increase in spine density that accompanied the stronger memory in mice microinjected with the GFP vector was prevented by increasing MEF2 function after training. Therefore, the formation of a spatial memory (and the associated increase in spine density) was blocked if MEF2 function was increased during training, and a post-training process that strengthens memory and resembles memory incubation (and the associated increase in spine density) was blocked if MEF2 function was increased shortly after training. These results agree with recent findings that increasing MEF2 function in the cortex shortly after context fear training similarly disrupts memory consolidation<sup>46</sup> and suggest that the ongoing refinement of spines is important for memory strengthening and/or maintenance.

The formation of a memory is thought to critically depend on transcription and *de novo* protein synthesis<sup>47</sup>. Recently, however, it has been suggested that protein degradation is also involved in synaptic plasticity and memory formation<sup>48,49</sup>. We observed that formation of either a spatial or fear memory was associated with a decrease in MEF2A and MEF2D protein levels. Although we believe we are the first to identify a role for MEF2 degradation in memory formation, degradation of neural MEF2 by a caspase-dependent process has been previously reported<sup>50</sup>.

Our results suggest that MEF2-mediated transcription normally constrains memory formation. We examined this by decreasing MEF2 function and training mice under weak (subthreshold) conditions. Disrupting MEF2 function (either by expressing dnMEF2 or knocking down endogenous protein by RNA interference) facilitated memory formation across two different paradigms (water-maze and auditory fear memory). These findings indicate that MEF2 has a bidirectional effect on memory formation, with MEF2-mediated transcription repressing memory formation.

MEF2 may suppress memory formation by activating the transcription of genes that encode proteins that weaken the excitatory synaptic transmission likely required for memory formation. For instance, *Arc* is an activity-dependent MEF2 target gene<sup>10</sup> whose protein product decreases the surface expression of AMPAR<sup>11,12</sup>. We found that specifically disrupting GluA2-containing AMPAR endocytosis at the time of training rescued the memory deficits produced by overexpressing MEF2. These results suggest that excessive internalization of AMPAR may be a critical mechanism mediating the memory deficits produced by MEF2.

MEF2 and several MEF2 target genes are implicated in human cognitive and psychiatric disorders<sup>10,13–15</sup>. Our results suggest that the cognitive deficits associated with these human disorders may be caused by a disruption of the MEF2-mediated gene network that regulates structural plasticity and memory formation. Our findings, that acutely manipulating MEF2 function in the adult brain produces robust effects on memory formation, raise the intriguing possibility that these human cognitive disorders may not result solely from untreatable developmental abnormalities but might be due to chronic dysregulation of the MEF2 function necessary for normal memory formation. Furthermore, our finding that the memory deficits produced by MEF2 were reversed by interfering with AMPAR endocytosis leads to the speculation that impaired AMPAR trafficking may contribute to this cognitive dysfunction and suggests a potential therapeutic target.

## METHODS

Methods and any associated references are available in the online version of the paper.

Note: Supplementary information is available in the online version of the paper.

## ACKNOWLEDGMENTS

We thank A. DeCristofaro, R. Braybon and M. Yamamoto for excellent technical assistance. This work was supported by grants from the Canadian Institutes of Health Research (CIHR; MOP-74650 (S.A.J.), MOP-86762 (P.W.F.)), EJLB Foundation (S.A.J.) and Natural Science and Engineering Research Council (S.A.J.). C.J.C., A.P.Y. and M.J.S. were supported by Restramp Fellowships (Hospital for Sick Children), A.P.Y. received support from the Alzheimer's Society of Canada, M.J.S. received a CIHR Frederick Banting and Charles Best Canada Graduate Scholarships Doctoral Award and a grant from the Faculty of Medicine at the University of Toronto, and C.J.C. received an Ontario Graduate Scholarship.

## AUTHOR CONTRIBUTIONS

S.A.J. and P.W.F. designed, directed and coordinated the study. C.J.C., V.M., L.R. and T.P. conducted behavioral experiments. C.J.C., A.P.Y. and M.J.S. performed the surgeries. C.J.C., V.M. and L.R. performed spine analysis. V.M., L.R. and G.V. performed immunohistochemistry. V.M. and P.J.R. conducted the cell culture experiments. C.J.C., V.M. and L.R. performed statistical analysis. J.-H.H. designed several constructs. R.L.N. generated viral vectors, shRNA and commented extensively on the design of experiments and use of viral vectors. S.A.J. and P.W.F. wrote the manuscript, with assistance from C.J.C., V.M. and L.R.

## COMPETING FINANCIAL INTERESTS

The authors declare no competing financial interests.

Published online at <http://www.nature.com/doi/10.1038/nn.3189>.

Reprints and permissions information is available online at <http://www.nature.com/reprints/index.html>.

- Bailey, C.H. & Kandel, E.R. Structural changes accompanying memory storage. *Annu. Rev. Physiol.* **55**, 397–426 (1993).
- Harris, K.M. & Stevens, J.K. Dendritic spines of rat cerebellar Purkinje cells: serial electron microscopy with reference to their biophysical characteristics. *J. Neurosci.* **8**, 4455–4469 (1988).
- Nimchinsky, E.A., Sabatini, B.L. & Svoboda, K. Structure and function of dendritic spines. *Annu. Rev. Physiol.* **64**, 313–353 (2002).
- Alberini, C.M. Transcription factors in long-term memory and synaptic plasticity. *Physiol. Rev.* **89**, 121–145 (2009).
- Abel, T., Martin, K.C., Bartsch, D. & Kandel, E.R. Memory suppressor genes: inhibitory constraints on the storage of long-term memory. *Science* **279**, 338–341 (1998).
- Flavell, S.W. *et al.* Activity-dependent regulation of MEF2 transcription factors suppresses excitatory synapse number. *Science* **311**, 1008–1012 (2006).
- Barbosa, A.C. *et al.* MEF2C, a transcription factor that facilitates learning and memory by negative regulation of synapse numbers and function. *Proc. Natl. Acad. Sci. USA* **105**, 9391–9396 (2008).
- Pulipparacharuvil, S. *et al.* Cocaine regulates MEF2 to control synaptic and behavioral plasticity. *Neuron* **59**, 621–633 (2008).
- Lyons, G.E., Micales, B.K., Schwarz, J., Martin, J.F. & Olson, E.N. Expression of *mef2* genes in the mouse central nervous system suggests a role in neuronal maturation. *J. Neurosci.* **15**, 5727–5738 (1995).
- Flavell, S.W. *et al.* Genome-wide analysis of MEF2 transcriptional program reveals synaptic target genes and neuronal activity-dependent polyadenylation site selection. *Neuron* **60**, 1022–1038 (2008).
- Chowdhury, S. *et al.* *Arc/Arg3.1* interacts with the endocytic machinery to regulate AMPA receptor trafficking. *Neuron* **52**, 445–459 (2006).
- Shepherd, J.D. *et al.* *Arc/Arg3.1* mediates homeostatic synaptic scaling of AMPA receptors. *Neuron* **52**, 475–484 (2006).
- Morrow, E.M. *et al.* Identifying autism loci and genes by tracing recent shared ancestry. *Science* **321**, 218–223 (2008).
- Greer, P.L. *et al.* The Angelman syndrome protein Ube3A regulates synapse development by ubiquitinating *arc*. *Cell* **140**, 704–716 (2010).
- Le Meur, N. *et al.* MEF2C haploinsufficiency caused by either microdeletion of the 5q14.3 region or mutation is responsible for severe mental retardation with stereotypic movements, epilepsy and/or cerebral malformations. *J. Med. Genet.* **47**, 22–29 (2010).
- McNaughton, B.L., Barnes, C.A., Meltzer, J. & Sutherland, R.J. Hippocampal granule cells are necessary for normal spatial learning but not for spatially-selective pyramidal cell discharge. *Exp. Brain Res.* **76**, 485–496 (1989).
- LeDoux, J.E. Emotion circuits in the brain. *Annu. Rev. Neurosci.* **23**, 155–184 (2000).
- Davis, M. The role of the amygdala in fear and anxiety. *Annu. Rev. Neurosci.* **15**, 353–375 (1992).
- Fanselow, M.S. & Gale, G.D. The amygdala, fear, and memory. *Ann. NY Acad. Sci.* **985**, 125–134 (2003).

20. Black, B.L. & Olson, E.N. Transcriptional control of muscle development by myocyte enhancer factor-2 (MEF2) proteins. *Annu. Rev. Cell Dev. Biol.* **14**, 167–196 (1998).
21. Pfeiffer, B.E. *et al.* Fragile X mental retardation protein is required for synapse elimination by the activity-dependent transcription factor MEF2. *Neuron* **66**, 191–197 (2010).
22. Chawla, M.K. *et al.* Sparse, environmentally selective expression of Arc RNA in the upper blade of the rodent fascia dentata by brief spatial experience. *Hippocampus* **15**, 579–586 (2005).
23. Frankland, P.W. *et al.* Consolidation of CS and US representations in associative fear conditioning. *Hippocampus* **14**, 557–569 (2004).
24. Wiltgen, B.J., Sanders, M.J., Anagnostaras, S.G., Sage, J.R. & Fanselow, M.S. Context fear learning in the absence of the hippocampus. *J. Neurosci.* **26**, 5484–5491 (2006).
25. Neely, M.D. *et al.* Localization of myocyte enhancer factor 2 in the rodent forebrain: regionally-specific cytoplasmic expression of MEF2A. *Brain Res.* **1274**, 55–65 (2009).
26. Sekeres, M.J., Neve, R.L., Frankland, P.W. & Josselyn, S.A. Dorsal hippocampal CREB is both necessary and sufficient for spatial memory. *Learn. Mem.* **17**, 280–283 (2010).
27. Josselyn, S.A. *et al.* Long-term memory is facilitated by cAMP response element-binding protein overexpression in the amygdala. *J. Neurosci.* **21**, 2404–2412 (2001).
28. McDonald, R.J. & White, N.M. A triple dissociation of memory systems: hippocampus, amygdala, and dorsal striatum. *Behav. Neurosci.* **107**, 3–22 (1993).
29. Moser, M.B., Trommald, M. & Andersen, P. An increase in dendritic spine density on hippocampal CA1 pyramidal cells following spatial learning in adult rats suggests the formation of new synapses. *Proc. Natl. Acad. Sci. USA* **91**, 12673–12675 (1994).
30. O'Malley, A., O'Connell, C. & Regan, C.M. Ultrastructural analysis reveals avoidance conditioning to induce a transient increase in hippocampal dentate spine density in the 6 hour post-training period of consolidation. *Neuroscience* **87**, 607–613 (1998).
31. Buzsáki, G. The hippocampo-neocortical dialogue. *Cereb. Cortex* **6**, 81–92 (1996).
32. Wilson, M.A. & McNaughton, B.L. Reactivation of hippocampal ensemble memories during sleep. *Science* **265**, 676–679 (1994).
33. Shen, J., Kudrimoti, H.S., McNaughton, B.L. & Barnes, C.A. Reactivation of neuronal ensembles in hippocampal dentate gyrus during sleep after spatial experience. *J. Sleep Res.* **7** (suppl. 1), 6–16 (1998).
34. Bunch, M.E. & Magdisck, W.K. The retention in rats of an incompletely learned maze solution for short intervals of time. *J. Comp. Psychol.* **16**, 385–409 (1933).
35. Shepherd, J.D. & Bear, M.F. New views of Arc, a master regulator of synaptic plasticity. *Nat. Neurosci.* **14**, 279–284 (2011).
36. Rial Verde, E.M., Lee-Osbourne, J., Worley, P.F., Malinow, R. & Cline, H.T. Increased expression of the immediate-early gene *arc/arg3.1* reduces AMPA receptor-mediated synaptic transmission. *Neuron* **52**, 461–474 (2006).
37. Collingridge, G.L., Isaac, J.T. & Wang, Y.T. Receptor trafficking and synaptic plasticity. *Nat. Rev. Neurosci.* **5**, 952–962 (2004).
38. Malinow, R. & Malenka, R.C. AMPA receptor trafficking and synaptic plasticity. *Annu. Rev. Neurosci.* **25**, 103–126 (2002).
39. Gainey, M.A., Hurvitz-Wolff, J.R., Lambo, M.E. & Turrigiano, G.G. Synaptic scaling requires the GluR2 subunit of the AMPA receptor. *J. Neurosci.* **29**, 6479–6489 (2009).
40. Brebner, K. *et al.* Nucleus accumbens long-term depression and the expression of behavioral sensitization. *Science* **310**, 1340–1343 (2005).
41. Miguez, P.V. *et al.* PKMzeta maintains memories by regulating GluR2-dependent AMPA receptor trafficking. *Nat. Neurosci.* **13**, 630–634 (2010).
42. Li, H. *et al.* Transcription factor MEF2C influences neural stem/progenitor cell differentiation and maturation *in vivo*. *Proc. Natl. Acad. Sci. USA* **105**, 9397–9402 (2008).
43. Cajal, S.R. Sur les ganglions et plexus nerveux de l'intestin. *C. R. Soc. Biol. (Paris)* **45**, 217–223 (1893).
44. Simon, D.J. *et al.* The microRNA miR-1 regulates a MEF-2-dependent retrograde signal at neuromuscular junctions. *Cell* **133**, 903–915 (2008).
45. Pickens, C.L., Golden, S.A., Adams-Deutsch, T., Nair, S.G. & Shaham, Y. Long-lasting incubation of conditioned fear in rats. *Biol. Psychiatry* **65**, 881–886 (2009).
46. Vetere, G. *et al.* Spine growth in the anterior cingulate cortex is necessary for the consolidation of contextual fear memory. *Proc. Natl. Acad. Sci. USA* **108**, 8456–8460 (2011).
47. Kandel, E.R. The biology of memory: a forty-year perspective. *J. Neurosci.* **29**, 12748–12756 (2009).
48. Ehlers, M.D. Activity level controls postsynaptic composition and signaling via the ubiquitin-proteasome system. *Nat. Neurosci.* **6**, 231–242 (2003).
49. Fioravante, D. & Byrne, J.H. Protein degradation and memory formation. *Brain Res. Bull.* **85**, 14–20 (2011).
50. Yang, Q. *et al.* Regulation of neuronal survival factor MEF2D by chaperone-mediated autophagy. *Science* **323**, 124–127 (2009).

## ONLINE METHODS

**Mice.** Male and female (2–4 months of age) F1 hybrid (C57Bl/6N Tac × 129S6/SvEv Tac) mice were group-housed (3–5 per cage) on a 12-h light-dark cycle. Experiments were conducted during light phase. Food and water were available *ad libitum*. Procedures were approved by The Hospital for Sick Children Animal Care and Use Committee in accordance with Canadian Council on Animal Care and US National Institutes of Health guidelines.

**Immunohistochemistry.** Male mice were handled daily (7 d), perfused with paraformaldehyde (4% PFA) and brains were sliced (50  $\mu\text{m}$ , coronal). Sections were counterstained with DAPI.

**pMEF2 immunohistochemistry: water maze.** Mice were trained in water maze ( $n = 4$ ) or maintained in home cage ( $n = 2$ ) and perfused 30 min after a probe test.

**pMEF2 immunohistochemistry: tone fear conditioning.** Mice were divided into treatment groups: (i) tone plus unconditioned stimulus (shock), tone fear conditioning ( $n = 4$ ), (ii) tone alone ( $n = 3$ ), (iii) immediate shock ( $n = 4$ ), and (iv) home cage ( $n = 3$ ). Tone plus unconditioned stimulus mice were placed in a conditioning chamber and 2 min later presented a tone (2,800 Hz, 85 dB, 30 s) that terminated with shock (0.5 mA, 2 s). Tone-alone mice were treated identically, except no shock was delivered. Immediate shock mice received shock (0.5 mA) without tone, 2 s after placement. Mice were perfused 30 min after training.

**pMEF2 immunohistochemistry: quantification.** A single image was acquired for dentate gyrus (optical slicing: 15  $\mu\text{m}$ , Zeiss LSM710); image stack for lateral amygdala (6 slices, 5- $\mu\text{m}$  step). Lateral amygdala was analyzed on a z-projection (optical slicing, 15  $\mu\text{m}$ ). Regions of interest (upper blade of the dentate gyrus, lateral amygdala) were delineated using DAPI (ImageJ). pMEF2 signal intensity from single neurons (DAPI<sup>+</sup> nuclei with diameter > 6.23  $\mu\text{m}$ ) was calculated as percent of background intensity (pMEF2 intensity in glial cells (nucleus diameter < 6.23  $\mu\text{m}$ )) and plotted as cumulative percentage. Nonparametric Kolmogorov-Smirnov tests were followed by pair-wise comparisons ( $\alpha = 0.01$  for multiple comparisons)<sup>51</sup>.

**Western blot.** Tissue was homogenized in cell lysis buffer and phosphate inhibitors as previously described<sup>52</sup>. Bands were visualized by exposure to film after treatment with ECL Western Blotting Detection Reagents (GE Healthcare). Optical intensity of bands associated with proteins of interest was measured relative to their respective GAPDH bands on the same blot (Image J).

**pMEF2 western blots: water maze.** Dentate gyrus and CA1 region of dorsal hippocampus was isolated 30–90 min after probe test in water maze-trained (trained,  $n = 9$ ) or home-cage mice ( $n = 9$ ). Blots were prepared as described above.

**pMEF2 western blots: context fear conditioning.** Mice were trained for context fear conditioning (3 × 0.5 mA shock; trained) or maintained in the home cage. Dentate gyrus and CA1 region of dorsal hippocampus was isolated 90 min or 6 h after training (pMEF2: home cage  $n = 4$ , 90 min  $n = 4$ , 6 h  $n = 4$ ; MEF2A; home cage  $n = 12$ , 90 min  $n = 9$ , 6 h  $n = 9$ ; and MEF2D: home cage  $n = 8$ , 90 min  $n = 7$ , 6 h  $n = 7$ ). Blots were prepared as described above.

**Arc western blot on primary hippocampal neurons.** Primary hippocampal neurons (12–14 d *in vitro* (DIV)) were prepared from embryonic day (E)18–19 mice<sup>53</sup> and infected with MEF2 vector, vector expressing shRNA to *Mef2a* and *Mef2d* or GFP vector by incubating neurons (5 h) in culture medium with viral particles. Twenty-four hours later, TTX (1  $\mu\text{M}$ ) and AP5 (100  $\mu\text{M}$ ) were added 1 h before KCl depolarization with 31% depolarization buffer (170 mM KCl, 2 mM CaCl<sub>2</sub>, 1 mM MgCl<sub>2</sub> and 10 mM HEPES) to culture medium for 4 h. Cells were homogenized in cell lysis buffer and western blot was performed.

**Primary antibodies.** Primary antibodies included antibodies to GAPDH (1:5,000, Cell Signaling 14C10), phospho-Ser408 MEF2A (1:1,000; provided by M.E. Greenberg), Arc (1:1,000, Synaptic Systems 156003), MEF2 (1:1,000; C-21; Santa Cruz), MEF2D (1:1,000; BD Bioscience 610774) and GFP (1:300, Millipore A11122).

**Luciferase reporter gene assays.** Gli36 cells (5 × 10<sup>4</sup>, provided by A. Epstein) were seeded in 24-well plates, and co-transfected (Lipofectamine 2000, OptiMEM, Invitrogen) with 100 ng MRE-reporter plasmid (pGL3-TATA-DesMEF; provided by E. Olson), 50 ng transfection-normalization plasmid CMV-lacZ (provided by J. McGlade) and 500 ng p1005+-derived plasmids expressing GFP alone, MEF2-VP16 or MEF2 $\Delta$ -VP16. Forty-eight hours after transfection, cells were

lysed (Reporter Lysis Buffer, Promega). Luciferase expression was determined using Firefly Luciferase Assay System (Promega), *lacZ* expression determined using ortho-nitrophenyl- $\beta$ -galactoside-based colorimetric  $\beta$ -galactosidase assay. Luciferase expression was normalized to *lacZ* expression within each experiment. Transfections were performed in duplicate within each experiment,  $n = 6$  for each group.

Primary hippocampal neurons (DIV 4, 24-well plates) were co-transfected (Lipofectamine 2000) with MRE- (500 ng) or CRE-reporter plasmid (500 ng) and TK-pRL vector (expressing *Renilla* luciferase (250 ng; Promega) to normalize transfection efficiency). Twenty-four h later, neurons were infected with GFP or MEF2 virus. Twenty-four hours later, TTX (1  $\mu\text{M}$ ) and AP5 (100  $\mu\text{M}$ ) were added 1 h before KCl depolarization with 31% depolarization buffer (170 mM KCl, 2 mM CaCl<sub>2</sub>, 1 mM MgCl<sub>2</sub> and 10 mM HEPES) for 4 h. Neurons were lysed and lysate (30  $\mu\text{l}$ ) assayed using Dual Luciferase Assay kit (Promega). Firefly and *Renilla* luciferase activity levels were quantified and raw data from MRE- or CRE-reporter assay divided by TK-pRL luciferase activity. Data represent means from independent experiments, with internal duplicates or triplicates for each condition,  $n = 8$  (MRE),  $n = 6$  (CRE).

**Arc mRNA fluorescence *in situ* hybridization (FISH).** Hippocampal neurons (DIV 10–12, 24-well plates) were transfected with GFP or MEF2 plasmids (Lipofectamine 2000). Twenty-four hours later, TTX (1  $\mu\text{M}$ ) and AP5 (100  $\mu\text{M}$ ) were added 1 h before 31% KCl depolarization buffer and forskolin (FSK, 30  $\mu\text{M}$ ) for 2 h. Neurons were fixed (4% PFA, 10 min), treated with acetic anhydride (10 min) and methanol/acetone solution (90 s). Coverslips were incubated with pre-hybridization buffer (Sigma, 1 h, 56 °C) and Arc-DIG riboprobe (100 ng) in hybridization buffer overnight (56 °C). Neurons were incubated 16–18 h later with 1% H<sub>2</sub>O<sub>2</sub> (30 min). FISH signal was detected by incubation with HRP-DIG (1:300, Jackson ImmunoResearch, 1 h, room temperature), amplified (TSA-bio, 30 min), incubated in streptavidin-Alexa Fluor 568 (1:300, Invitrogen, 1 h) and then incubated with blocking solution (30 min, room temperature). Images were acquired (Zeiss LSM710); single transfected neurons were traced (GFP channel) and FISH quantified within selected area (ImageJ).

**HSV vectors.** Plasmids encoding MEF2-VP16, MEF2 $\Delta$ -VP16 were provided by M.E. Greenberg<sup>6</sup>, and plasmids encoding dnMEF2 were provided by I. Skerjanc<sup>54</sup> (Supplementary Fig. 2a). All constructs were subcloned into bicistronic pHSV-p1005+ amplicons expressing GFP alone or with MEF2 constructs. tGFP-shRNAmir against *Mef2a* (oligo identifier V3LHS\_319382; Thermo Scientific) and MEF2D (V2LHS\_200022) were subcloned from lentivirus encoding human GIPZs vectors (Thermo Scientific) into pHSV-p1005+ amplicons. Vectors were prepared according to published methods<sup>55,56</sup>.

**Validation of shRNA-mediated *Mef2* knockdown.** MEF2A and MEF2D expression was assessed by immunofluorescence in hippocampal primary neurons (10–12 DIV) transfected with shRNA directed against *Mef2a* and *Mef2d*. Neurons were fixed (4% PFA, 20 min) and coverslips incubated with antibodies. Fluorescence intensity of staining for MEF2A and MEF2D proteins was quantified (ImageJ).

**Vector-induced toxicity.** MTT (3-(4,5-dimethylthiazol-2-yl)-2,5-diphenyltetrazolium bromide) assays<sup>53,57</sup> were used to investigate potential viral toxicity. Hippocampal neurons (DIV 12–14) were infected with vector (GFP, MEF2, MEF2A or dnMEF2 vector) for 5 h. MTT solution (10% v/v culture medium volume) was added 24–30 h later (3 h, 37 °C). At least four samples for each condition were quantified. Spectrophotometer measurements were compared to those for similar non-infected cultures ( $n = 4$  independent cultures for each group). As a control, we treated additional hippocampal neurons with increasing levels of 0.1 M PBS (control, 2 × 1 min 0.1 M PBS, 2 × 3 min 0.1 M PBS, 2 × 6 min 0.1 M PBS) to verify neuronal viability ( $n = 6$  independent cultures for each group).

**AAV vector.** Plasmids encoding shRNA to *Mef2a* and shRNA *Mef2d* were provided by M.E. Greenberg. Constructs were packaged into AAV<sub>9</sub> vector (AAV<sub>9</sub>-CAG-GFP-H1-MEF2A-RNAi, AAV<sub>9</sub>-CAG-GFP-H1-MEF2D-RNAi) by Virovek (<http://www.virovek.com/>).

**Surgery.** Mice were pretreated with atropine sulfate (0.1 mg/kg, intraperitoneal), anesthetized with chloral hydrate (400 mg/kg, intraperitoneal) and placed in stereotaxic frame. Holes were drilled above the dentate gyrus (AP = -2.0 mm,

ML =  $\pm$  2.0 mm, DV = -2.0 mm from bregma) or lateral amygdala (AP = -1.4 mm, ML =  $\pm$  3.5 mm, DV = -5.0 mm)<sup>58</sup>. Bilateral microinjections of HSV (2.0  $\mu$ l for dentate gyrus; 1.5  $\mu$ l for lateral amygdala) were delivered over 20 min through glass micropipettes. Volume of AAV<sub>9</sub> vector microinjection was 0.3  $\mu$ l. Because transgene expression using HSV viral system peaks 3 d after surgery<sup>27</sup>, we trained mice 2 d after surgery in water-maze experiments (except where specified). In fear conditioning experiments, mice were trained 2 d after HSV microinjection. Mice with AAV<sub>9</sub> were trained between 10–21 d after microinjection.

**Histology.** Placement or extent of viral infection for each mouse was determined using GFP immunofluorescence by an examiner unaware of behavioral data. Four days after HSV microinjection, mice were perfused and mouse brains were sliced. Only mice with strong bilateral GFP expression in target region ('bilateral hit') were included in subsequent data analysis.

**Water maze-based testing of spatial memory.** Training and testing in the water maze were conducted as previously described<sup>59,60</sup>. For strong training, mice received two blocks of three trials per day, for 3 d. For weak training (Fig. 6), mice received one block of three trials per day, for 3 d. Sixty min after final training trial, spatial memory was assessed in a probe test during which the platform was removed from the pool and the mouse allowed to search for 60 s. Behavioral data were acquired and analyzed using Actimetrics software. During training, we analyzed escape latency, swim speed and thigmotaxic behavior (time mice spent within 5 cm of pool wall). In the probe test, we quantified spatial memory by measuring amount of time mice spent searching in target zone (20 cm radius, centered on location of platform during training; 11% of pool surface) versus average time spent in three other equivalent zones in other areas of pool.

**Statistical analysis.** We analyzed the time required to reach the platform (escape latency) using a two-way analysis of variance (ANOVA) with between-group factor 'vector' and within-group factor 'day' (3 d). An ANOVA (vector) was used to analyze overall swim speed and thigmotaxis averaged over training. For the probe test, we first quantified spatial bias by comparing amount of time mice spent in target zone versus average time spent in equivalent zones in 'other' three quadrants of the pool using an ANOVA (between-subjects variable vector, within-subjects variable zone (target, others)). Next, we analyzed time spent in target zone between groups using one-way ANOVA (vector). Significant effects were further analyzed with Newman-Keuls post-hoc tests.

**Fear memory testing.** Mice were trained as above. Context fear testing occurred 24 h after training, and tone fear testing occurred 48 h after training. For context fear testing, mice were placed in conditioning context and the amount of time spent freezing (cessation of all movement except for respiration) during 5-min test was assessed (Actimetrics). For auditory (tone) fear testing, mice were placed in a new chamber and, 2 min later, tone was presented (1 min). Freezing before and during tone was assessed.

**Dendritic spine analysis.** Brain slices (50  $\mu$ m, from random subset of mice, Fig. 2c) were stained and imaged<sup>52</sup>. Neurons were chosen for tracing based on morphology (elliptical cell body, unipolar dendritic tree signifying granule cell), location (upper blade dentate gyrus), isolation and general appearance (no dendritic truncations). Reconstructed neurons were analyzed (NeuroLucida Explorer)<sup>52</sup>. Spine density (protrusions in direct contact with dendritic shaft) per 10  $\mu$ m of dendrite was averaged per mouse. Neurons and mice in each group; home cage, GFP (11 neurons from 5 mice); home cage, MEF2 (15 neurons, 5 mice); home cage, MEF2 $\Delta$  (10 neurons, 5 mice); trained, GFP (14 neurons, 7 mice); trained, MEF2 (15 neurons, 8 mice); trained, MEF2 $\Delta$  (14 neurons, 6 mice); after training, GFP (incubation experiment, 13 neurons, 5 mice); and after training, MEF2 (16 neurons, 7 mice).

To determine whether effects of increasing MEF2 function on spine growth were a cell-autonomous or circuit property, we examined effects of MEF2 vector on neighboring 'control non-infected' neurons. We microinjected mice with two vectors, each expressing a different fluorescence marker (green or red). 'Green' vector expressed either MEF2-GFP or GFP alone. 'Red' vector expressed tandem dimmer (td)Tomato alone (just used as a fluorescence marker to allow assessment of spine density) (Supplementary Fig. 4b). Mice were trained in the water maze or not.

**TAT-GluA2<sub>3Y</sub> peptide.** To disrupt GluA2-containing AMPAR endocytosis, we used an interference peptide derived from the C-terminal tail of GluA2 (GluA2<sub>3Y</sub>, 869YKEGYNVYG<sup>877</sup>)<sup>40</sup>. TAT-GluA2<sub>3Y</sub> and TAT-only control protein (GenScript) were dissolved in saline and administered (1.5  $\mu$ mol/g, intraperitoneally) 1 h before training.

- Keppel, G. & Wickens, T.D. *Design and Analysis: A Researcher's Handbook* 4th edn. (Prentice Hall, 2004).
- Yiu, A.P., Rashid, A.J. & Josselyn, S.A. Increasing CREB function in the CA1 region of dorsal hippocampus rescues the spatial memory deficits in a mouse model of Alzheimer's disease. *Neuropsychopharmacology* **36**, 2169–2186 (2011).
- Zalfa, F. *et al.* A new function for the fragile X mental retardation protein in regulation of PSD-95 mRNA stability. *Nat. Neurosci.* **10**, 578–587 (2007).
- Karamboulas, C. *et al.* Disruption of MEF2 activity in cardiomyoblasts inhibits cardiomyogenesis. *J. Cell Sci.* **119**, 4315–4321 (2006).
- Russo, S.J. *et al.* Nuclear factor kappa B signaling regulates neuronal morphology and cocaine reward. *J. Neurosci.* **29**, 3529–3537 (2009).
- Clark, M.S. *et al.* Overexpression of 5-HT1B receptor in dorsal raphe nucleus using Herpes Simplex Virus gene transfer increases anxiety behavior after inescapable stress. *J. Neurosci.* **22**, 4550–4562 (2002).
- Miller, R.R. & McDevitt, C.A. A quantitative microwell assay for chondrocyte cell adhesion. *Anal. Biochem.* **192**, 380–383 (1991).
- Paxinos, G. & Franklin, K.B.J. *The Mouse Brain in Stereotaxic Coordinates*, 2nd edn. (Academic Press, San Diego, 2001).
- Teixeira, C.M., Pomedli, S.R., Maei, H.R., Kee, N. & Frankland, P.W. Involvement of the anterior cingulate cortex in the expression of remote spatial memory. *J. Neurosci.* **26**, 7555–7564 (2006).
- Maei, H.R., Zaslavsky, K., Teixeira, C.M. & Frankland, P.W. What is the most sensitive measure of water maze probe test performance? *Front. Integr. Neurosci.* **3**, 4 (2009).